Journal of Medicinal Chemistry

ARTICLE

pubs.acs.org/jmc

Effects of Cyclization on Stability, Structure, and Activity of α-Conotoxin RgIA at the α9α10 Nicotinic Acetylcholine Receptor and $GABA_B$ Receptor

Reena Halai,[†] Brid Callaghan,[‡,§] Norelle L. Daly,[†] Richard J. Clark,[†,∥] David J. Adams,[‡,§] and David J. Craik*[,†]

[†]Institute for Molecular Bioscience, Division of Chemistry and Structural Biology and [‡]Queensland Brain Institute, The University of Queensland, Brisbane, Queensland 4072, Australia

[§]Health Innovations Research Institute, RMIT University, Melbourne, Victoria 3083, Australia

Supporting Information

ABSTRACT: α-Conotoxin RgIA is of interest as a lead in the development of drugs for neuropathic pain. It modulates the α9α10 nicotinic acetylcholine receptor (nAChR) and the $GABA_B$ receptor, both of which are implicated in antinociception. However, because of its peptidic nature, RgIA is potentially susceptible to generic problems encountered by peptide-based drugs of poor oral bioavailability, short biological half-life, and low stability. Here, we improved the biopharmaceutical properties of RgIA by backbone cyclization using 3−7 residue peptidic linkers. Cyclization with a six-residue linker does not perturb the overall structure of RgIA, improves selectivity for the $GABA_B$ receptor over the α9α10 nAChR, and improves stability in human serum. The results provide insights to further improve the therapeutic properties of RgIA and other conotoxins being considered as drug leads and confirm that cyclization is a readily applicable strategy to improve the stability of peptides with proximate N- and C-termini.

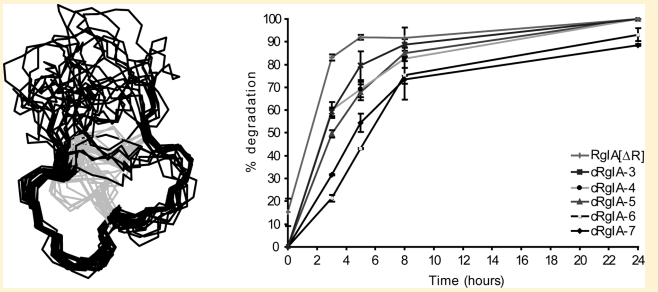

INTRODUCTION

The venoms of marine snails provide a plethora of conotoxins that have promising potential as drug leads based on their selectivity and potency toward therapeutically relevant membrane receptors and ion channels.[1−5] Several conotoxins are at various stages of preclinical or clinical development, with one example, ω-conotoxin MVIIA, approved since 2004 for the treatment of neuropathic pain.[6] However, owing to their peptidic nature, conotoxins potentially are susceptible to the general disadvantages of peptide-based drug leads in vivo, including poor stability, low oral bioavailability, and short biological half-life.[7] In one approach to overcoming these limitations, synthetic backbone cyclization of conotoxins, with appropriately sized linkers spanning the N- and the C-termini, has been used to engineer improved stability against a proteolytic attack and associated degradation in human serum, while maintaining biological activity. This approach has been successfully demonstrated for several conotoxins, including MII, MrIA, and Vc1.1,[8−10] and potentially is applicable to other conotoxins. Here, we aimed to apply cyclization technology to a conotoxin with a different Cys framework from these to test the generality of the approach and herein report studies on conotoxin RgIA. This peptide is of potential interest as a lead for the development of new treatments for chronic pain.[11,12]

RgIA is a member of the 4/3 subfamily of α-conotoxins, with the numerals 4/3 referring to the number of residues in the first and second cysteine loops,[13,14] respectively (Figure 1). This 4/3 spacing contrasts with the 4/7 spacing of α-conotoxins MII and Vc1.1, although all three peptides share a common disulfide connectivity characteristic of α-conotoxins, referred to as the globular connectivity. By contrast, χ-conotoxin MrIA has a disulfide connectivity different from that of the α-conotoxins, referred to as the ribbon form. Thus, RgIA differs either in Cys spacing or disulfide connectivity from other conotoxins that have been artificially cyclized, with the exception of a recent study on ImI, which also has a 4/3 framework.[15] However, the ImI study focused on short linkers (of three or fewer residues), which generally resulted in non-native disulfide isomers that were not tested for biological activity. Here, we focused on longer linkers of RgIA to favor the bioactive fold.

The sequence of RgIA was discovered using PCR amplification of a DNA template from *Conus regius*.[16] However, when the native peptide, reg1e, was isolated from the venom duct of *C. regius*, two major differences to RgIA were observed: (a) the putative C-terminal residue, Arg,[13] in RgIA was not present, and the peptide instead had an amidated C-terminus, a post-translational modification common to many other α-conotoxins, and (b) a hydroxyproline was present at position 6 instead of a proline.[17] The C-terminal Arg[13] has been reported not to play a

Received: August 7, 2011
Published: September 02, 2011

dx.doi.org/10.1021/jm201060r | *J. Med. Chem.* 2011, 54, 6984–6992

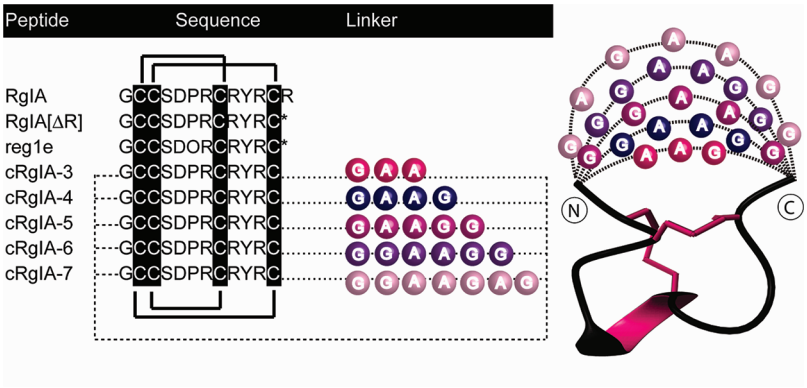

Figure 1. Covalent structure and sequences of RgIA and analogues. The cyclization strategy applied to RgIA is shown for different size linkers spanning the N- and C-termini of the peptide structure. The sequences of the analogues are shown with the cysteines marked with black bars. The black lines above the sequences indicate the native (globular)[50] disulfide connectivity of Cys^{I}-Cys^{III} and Cys^{II}-Cys^{IV}. The black lines below the sequence show the ribbon[50] disulfide connectivity of Cys^{I}-Cys^{IV} and Cys^{II}-Cys^{III}.

significant role in the binding or activity of RgIA at the $\alpha9\alpha10$ nicotinic acetylcholine receptor (nAChR).[18] Consequently, the cyclic analogues of RgIA described in the current study do not contain the C-terminal Arg[13] and are generically referred to as cRgIA-(n) analogues, where n refers to the number of residues in the linker.

Until recently, the presumed main target for RgIA and the α-conotoxin Vc1.1 was the $\alpha9\alpha10$ nAChR.[16,18,19] However, a recent study identified another potential target, the $GABA_B$ receptor coupled to the N-type calcium channel, in the antinociceptive effects of RgIA and Vc1.1.[11] The $\alpha9\alpha10$ nAChR is a ligand-gated ion channel with an important role in the auditory system, mediating synaptic transmission between efferent olivocochlear fibers and cochlear hair cells[20−22] and splanchnic nerve-chromaffin cell synapses in acute adrenal slices of cold-stressed rats.[23] In contrast, the $GABA_B$ receptor is a metabotropic receptor coupled to a G protein[24] and found to exist as a heterodimer of $GABA_{B1}$ and $GABA_{B2}$ subunits.[25−29] $GABA_B$ is distributed widely in the central and peripheral nervous systems and has been linked to antinociception and antidrug cravings.[30−32]

In this study, we used backbone cyclization to improve the serum stability of RgIA, while maintaining activity at the $\alpha9\alpha10$ nAChR and the $GABA_B$ receptor. A range of cyclic and linear analogues were synthesized, as summarized in Figure 1. The cyclic analogues were designed with three to seven residues in the linker region and were tested at the human $\alpha9$/rat $\alpha10$ nAChR hybrid and the $GABA_B$ receptor. The cyclic and equivalent linear analogues were also tested in human serum to examine the effect of cyclization on the biological half-life of the peptides. The structure of the most potent analogue was determined using NMR and provides a basis for understanding the improved stability and efficacy of the re-engineered native toxin.

RESULTS

Peptide Synthesis and Oxidative Folding. Peptide chains were assembled using 9-fluorenylmethyloxycarbonyl or *tert*-butoxycarbonyl chemistry for linear or cyclic peptides, respectively. The folding of linear RgIA was previously achieved with the addition of 25% propan-2-ol in 0.1 M NH_4HCO_3 folding buffer to favor the globular isomer and minimize the yield of unwanted ribbon isomer.[33] In the current study, all cyclic analogues were folded using a directed folding approach to explicitly form the desired disulfide bonds. Globular RgIA has two disulfide bonds, with a Cys^{I}-Cys^{III} and Cys^{II}-Cys^{IV} connectivity, so two acetamidomethyl (Acm) protected cysteines (Cys^{II} and Cys^{IV}) were incorporated into the linear precursors. This ensured that in the first folding step in 0.1 M NH_4HCO_3, the Cys^{I}-Cys^{III} disulfide bond would form, and after reaction with iodine, the second disulfide bond, Cys^{II}-Cys^{IV}, would form. Small yields of the ribbon isomer were also present (~5−10%), suggesting minor reshuffling of the disulfide bonds during the iodine oxidation step. The linear peptides reg1e and RgIA[ΔR] were folded in 0.1 M NH_4HCO_3 without the addition of 25% propan-2-ol and yielded two isomers in a 3:2 globular/ribbon ratio, similar to that found for RgIA in the presence of 25% propan-2-ol.[33] The isomers were identified by NMR, and the globular isomer was separated and purified for further studies. The ribbon isomer has previously been shown to be inactive[33] and was therefore not further examined.

NMR Analysis and Structure Determination. NMR spectroscopy was used to assess the structures of the cyclic peptides relative to the wild-type peptides, RgIA and RgIA[ΔR], and thereby to confirm the native globular fold. RgIA is reported to have a type I β-turn from Cys^{2}-Asp^{5}, a 3_{10} helix over residues Asp^{5}-Arg^{9}, and a type VIII β-turn for Arg^{9}-Cys.[12,33] For the cyclic peptides studied here, αH_i-NH_{i+1} NOE connectivities from NOESY spectra were used to guide the sequential assignment of the individual spin systems determined from TOCSY spectra. As αH secondary shifts are sensitive to the backbone conformation,[34] they were used to assess if there were any changes in the secondary structure caused by the head-to-tail cyclization of the various analogues. Figure 2A shows that the αH secondary shifts of most analogues superimpose well with those of RgIA and RgIA[ΔR], confirming that they have a native secondary structure. The linker region is, as expected, disordered based on small values for secondary shifts in this region. The secondary shifts of cRgIA-3 and cRgIA-4 showed some variations relative to RgIA-[ΔR], suggesting perturbations in their structures. In addition, there is a small localized variation in αH secondary shift at position 6 in reg1e, presumably due to the Pro^{6} at this position being replaced with hydroxyproline.[35]

Given the similarity of secondary shifts for most cyclic analogues, a full three dimensional (3D) structure was determined for only one example, i.e., cRgIA-6, using simulated annealing based on NMR-derived restraints. The NMR-derived structural ensemble is

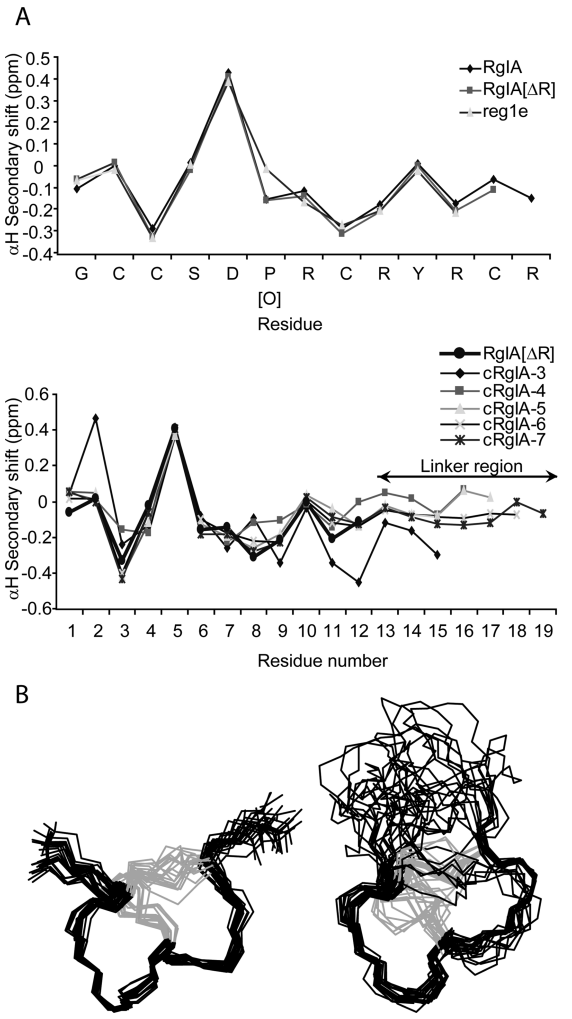

Figure 2. αH secondary shifts of RgIA and analogues with structures for RgIA and cRgIA-6. (A) αH secondary shifts for all the peptides synthesized in this study. There is a precise superimposition of the peptide backbone (residues 2−12) for most of the analogues relative to RgIA. Some structural perturbations are apparent for cRgIA-3 and -4. The linker region is indicated. (B) Ensembles of the NMR-derived structure are shown for RgIA and its cyclic analogue cRgIA-6. The peptide backbone is shown in black and the disulfide bonds in gray. The 20 lowest energy structures for RgIA are from Clark et al.,[33] and the 20 lowest energy structures of cRgIA-6 were determined in this study.

shown in Figure 2B, and the corresponding structural statistics are in Table 1. PROMOTIF[36] and PROCHECK[37] were used to analyze the ensemble of structures. Consistent with the linear wild-type peptide, a 3_{10} helix between residues 2−8 and a type IV β-turn between residues 9−12 were identified. The backbone rmsd for residues 2−11 is 0.88 Å, whereas the rmsd over only loop 1 (residues 2−7) is 0.34 Å, showing that loop 2 is somewhat disordered compared to the rest of the structure. By contrast, loop 2 is not disordered in RgIA (shown for comparison in Figure 2B). This minor difference between the linear and cyclic structures appears to be related to broadening of some peaks near Tyr[10] in the cRgIA-6 NMR spectra leading to fewer NOEs. For example, no cross-peaks involving the amide protons of Arg[9] and Tyr[10] were observed, and the HN-Hα cross-peak for Arg[11] was broadened compared to other cross-peaks in the spectra.

Table 1. NMR Statistics for cRgIA-6[a]

experimental data for cRgIA-6	
NMR Distance and Dihedral Constraints	
total NOE	47
sequential ($\|i-j\|=1$)	26
medium-range ($\|i-j\|\leq 4$)	13
long-range ($\|i-j\geq 5$)	8
φ restraints	3
Structure Statistics	
maximum dihedral angle violation (deg)	3
maximum distance constraint violation (Å)	0.3
Mean Energies (kJ/mol)	
$E_{overall}$	−522.29 ± 19.07
E_{bonds}	3.16 ± 0.82
E_{angles}	16.04 ± 4.78
$E_{improper}$	3.04 ± 1.18
E_{VDW}	−6.39 ± 7.95
E_{NOE}	3.89 ± 1.82
E_{cDIH}	0 ± 0
$E_{dihedral}$	57.21 ± 7.41
$E_{electrostatic}$	−599.25 ± 22.78
rmsd	
bonds (Å)	0.0037 ± 0.0005
angles (deg)	0.51 ± 0.07
improper (deg)	0.39 ± 0.07
NOE	0.032 ± 0.008
cDIH	0 ± 0
mean global backbone atoms (residues 2−11)	0.88 ± 0.38
mean global heavy atoms (residues 2−11)	2.40 ± 0.57
Ramachandran Statistics (%)	
residues in most favored regions	77
residues in additional allowed regions	23
residues in generously allowed regions	0
residue in disallowed regions	0

[a] Pairwise rmsd was calculated among 20 refined structures.

Potency of the RgIA Analogues at the Human α9/Rat α10 nAChR (hα9rα10). RgIA and all analogues were tested on the α9α10 (human α9/rat α10) nAChR. The EC_{50} for ACh activation of the hα9rα10 hybrid was ∼50 μM, and the IC_{50} for inhibition of ACh-evoked currents by RgIA was ∼50 nM (see Figure 3). The analogues were initially tested at a concentration of 50 nM, and the results statistically analyzed using a two-sample *t* test at p = 0.05 (assuming equal variances). This initial screen confirmed that RgIA and RgIA[ΔR] had no significant difference (60 ± 3.9% and 55 ± 5%, respectively) in their inhibitory activity at 50 nM. However, reg1e, cRgIA-3, cRgIA-4, cRgIA-5, and cRgIA-6 had significantly reduced inhibitory activities of 41 ± 14.7%, 8 ± 8.6%, 12 ± 7.2%, 25 ± 5.3%, and 39 ± 3.7%, respectively, relative to RgIA. Of the five cyclic analogues tested, cRgIA-7 was equally potent to RgIA[ΔR], causing 60 ± 5.7% inhibition of ACh-evoked currents. The IC_{50} was determined (Figure 3B) for the analogues that retained activity comparable to that of RgIA (RgIA[ΔR] and cRgIA-7), as they were of most interest for further study.

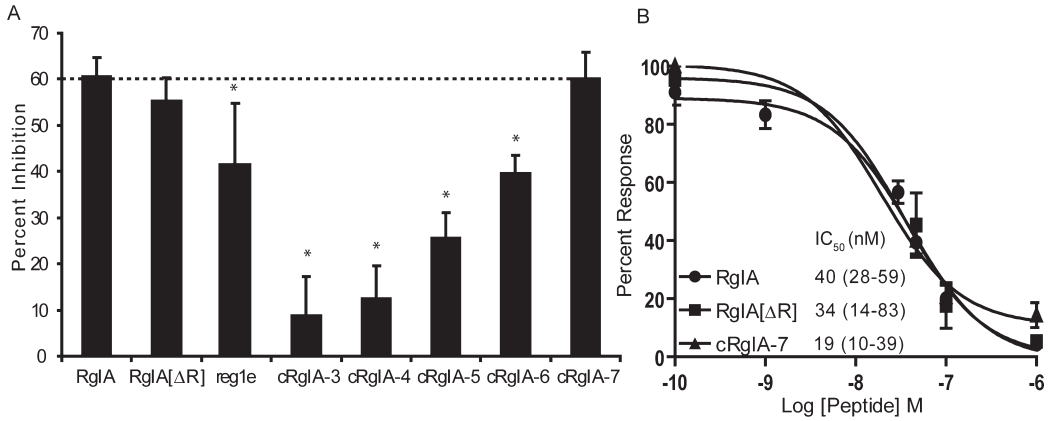

Figure 3. Inhibitory activity of RgIA analogues at the human $\alpha 9$/rat $\alpha 10$ nAChR expressed in *Xenopus* oocytes. (A) RgIA, RgIA[ΔR], and cRgIA-7 at a single dose of 50 nM exhibits comparable activity. Asterisks indicate analogues with significant reductions in their inhibition of ACh-evoked currents relative to RgIA. (B) Concentration−response curves and IC_{50}s obtained for RgIA, RgIA[ΔR], and cRgIA-7 (95% confidence intervals are indicated).

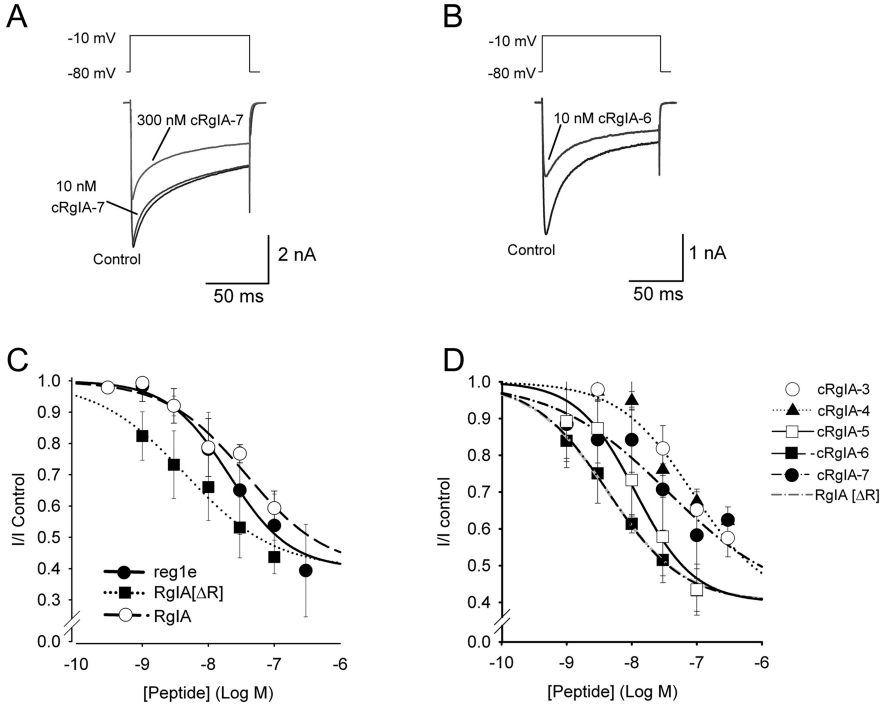

Figure 4. Effects of cyclic RgIA analogues at $GABA_B$ receptor-coupled HVA calcium channels in rat DRG neurons. Superimposed depolarization-activated whole cell Ba^{2+} currents elicited by voltage steps from a holding potential of −80 to −10 mV in the absence (control) and presence of (A) 10 nM and 300 nM cRgIA-7 and (B) 10 nM cRgIA-6, respectively. Concentration−response relationship for the inhibition of HVA Ca^{2+} channel currents in DRG neurons by (C) RgIA and linear analogues and (D) RgIA[ΔR] and cyclic RgIA analogues with 3−7 linkers (n = 2−5 cells per data point). Data points represent the mean ± SEM of normalized peak current amplitude.

Effects of RgIA and Cyclic Analogues on $GABA_B$ Receptor-Mediated Inhibition of High Voltage-Activated (HVA) Ca^{2+} Channels. On the basis of recent reports[11,38] implicating the $GABA_B$ receptor as a target for Vc1.1 and RgIA, the linear and cyclic analogues were tested for $GABA_B$ receptor-dependent inhibition of HVA Ca^{2+} channel currents in rat DRG neurons. As shown in Figure 4, the six-residue linker analogue was the most potent of the cyclic RgIA peptides. The IC_{50} for the obtained inhibition of HVA Ca^{2+} channel currents by RgIA, reg1e, RgIA[ΔR], cRgIA-3, cRgIA-4, cRgIA-5, cRgIA-6, and cRgIA-7 was 40.7 ± 13.7 nM (n = 3), 20.5 ± 7.5 nM (n = 3), 4.4 ± 2.3 nM (n = 4), 82.5 ± 17.5 nM (n = 3), 70.1 ± 12.0 nM (n = 3), 11.5 ± 4.6 nM (n = 4), 4.3 ± 1.4 nM (n = 4), and 36.3 ± 18.3 nM (n = 5), respectively. For convenience, comparative data for the $\alpha 9\alpha 10$ nAChR and $GABA_B$ receptors are summarized in Table 2.

Serum Stability Assay. RgIA[ΔR] and the cyclic analogues were tested in human serum to determine the effects of cyclization on stability. Figure 5 shows that the cyclic peptides are more stable than the corresponding linear peptide, with the six- and seven-residue linkers most effective. At 5 h, 92 ± 1.08% of the linear RgIA[ΔR] analogue had degraded, but only 43 ± 0.3% and 54 ± 4% (n = 3), respectively, of the cRgIA-6 and -7 linker analogues had degraded.

dx.doi.org/10.1021/jm201060r |*J. Med. Chem.* 2011, 54, 6984–6992

Table 2. Comparison of IC_{50}s (nM) Determined for Inhibition of $\alpha9\alpha10$ nAChRs and $GABA_B$/N-type Ca^{2+} Channels by RgIA and Analogues, RgIA[ΔR], cRgIA-6, and cRgIA-7[a]

peptide	$\alpha9\alpha10$ nAChR (n)	$GABA_B$/N-type Ca^{2+} channel (n)
RgIA	40 (28−59) (3)	40.7 ± 13.7 (3)
RgIA[ΔR]	34 (14−83) (3)	4.4 ± 2.3 (4)
cRgIA-6	>50 (3)	4.3 ± 1.4 (4)
cRgIA-7	19 (10−39) (3)	36.3 ± 18.3 (5)

[a] Confidence intervals (95%) are indicated for $\alpha9\alpha10$ nAChR and mean ± SEM for $GABA_B$/N-type Ca^{2+}.

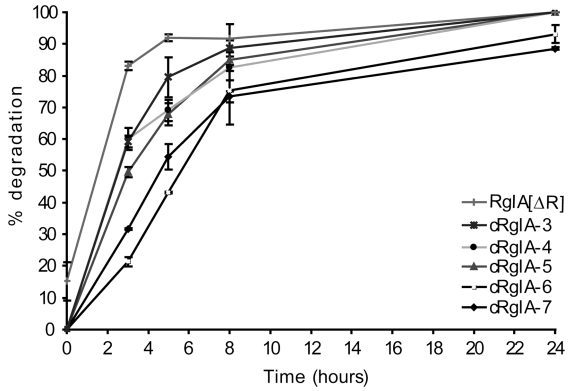

Figure 5. Serum stability of cyclic RgIA analogues. Cyclic and selected linear analogues were incubated in human serum over 24 h and their degradation monitored. The linear analogue, RgIA[ΔR], was the least stable, and as linker size of the cyclic analogue increased, so too did the stability of the peptides. The six-residue and seven-residue linker peptides are the most stable in human serum. Error bars represent the mean ± SEM.

DISCUSSION

In this study, we designed and synthesized a range of cyclic RgIA analogues with linkers ranging from three to seven residues to span the peptide termini of a native conotoxin sequence. The aim was to produce an analogue that maintained activity relative to RgIA but had improved biological half-life in human serum. NMR chemical shift analysis confirmed the structural conservation of the five- to seven-residue linker analogues relative to the linear peptide. The cyclic peptides were tested at the $\alpha9\alpha10$ nAChR and the $GABA_B$ receptor, and their stability in human serum was measured. The 3D structure of the most potent cyclic analogue, i.e., that containing a six-residue linker spanning the termini of the native peptide, was determined. Overall, the structure−activity data confirmed that the six- and seven-residue linker analogues maintain native structure and activity at the $GABA_B$ receptor and are significantly more stable than the linear peptide in human serum. The results highlight the value of cyclization for improving the biopharmaceutical properties of 4/3 α-conotoxin RgIA and more broadly provide guidance for cyclization strategies for other disulfide-rich proteins.

The cyclic RgIA peptides were designed taking into account the distance between the N- and C-termini of the native peptide, which is ∼11.6 Å. From previous studies on other α-conotoxins,[10,39] we deduced that a linker of six residues or more would be appropriate to span this distance. Although it was anticipated that smaller linkers (2−4 residues) might induce strain in the molecule, it was of interest to verify this experimentally. Thus, we synthesized a suite of cyclic RgIA[ΔR] analogues incorporating linkers of various lengths, including some shorter ones. The linkers were composed of mixtures of Gly and Ala residues, appropriately ordered to facilitate NMR spectral assignments. We reasoned that with no more than two consecutive residues of the same type present in the linker, there would be minimal overlap in the NMR spectra but that three or more consecutive residues of the same type might lead to chemical shift degeneracy, making structure determination more difficult. Gly and Ala were chosen as linker constituents primarily because they are small and do not have side chains capable of hydrogen bonding, and so are not likely to disrupt the native structure of RgIA or to form new secondary structural elements in the linker region.

As cyclization of the backbone could lead to structural perturbations, it was important to check the structures of the cyclic analogues prior to interpreting the biological activity data. Secondary αH NMR chemical shifts are sensitive to peptide conformations and were used to provide comparative information on the structural folds. The secondary αH shifts of the core regions of most of the cyclic analogues were very similar to those of RgIA, suggesting no change in the overall global fold of the peptides. Notable exceptions were cRgIA-3 and cRgIA-4, which exhibited significant variations in the secondary αH chemical shifts of core residues, suggesting perturbations in their overall backbone fold. Thus, the hypothesis that a linker of three or four residues is likely to force the N- and the C-termini together, putting strain on the peptide conformation, proved to be experimentally verified. Consistent with their perturbed conformations, these analogues had substantially decreased activities at both the $\alpha9\alpha10$ nAChR and the $GABA_B$ receptor. Overall, it is clear that linkers of five residues or more introduce minimal strain into the cyclic peptides, and we thus focused on these analogues.

The NMR αH chemical shifts of the linkers themselves were all close to random coil values, suggesting that the linkers do not have a defined conformation, a suggestion that was verified from the full 3D structure determination of cRgIA-6 (Figure 2B). This finding is consistent with the original design hypothesis that the Gly/Ala linkers would not adopt a well-defined structure, but its validation provides guidance for the optimization of the design of new cyclic peptides. Now that the principles governing linker length have been established and the chemical means of making cyclic conotoxins has been developed, it might be useful in future studies to consider more complex linkers. Most α-conotoxins should be tolerant to a wide range of linker types as their bioactive regions are all confined within the Cys-rich core, and the vast majority of α-conotoxins contain at most one N- or C-terminal residue outside that core.[40] They are thus not biased by pre-existing sequences in what will become the linker region. Conotoxin GID is a rare exception to this trend and has an extended N-terminal tail that appears to be important for activity.[41] In cases like GID, the existing residues in the N- or C-terminal tails could be incorporated within a cyclizing linker. More generally, linkers could be used to modify biopharmaceutical properties in a number of ways, including increasing membrane permeability by incorporating hydrophobic amino acids or by attaching glycolipids to linker residues.[42,43] Nonpeptidic linkers have also been contemplated.[44,45] The findings of the current study should assist in such future linker engineering studies since they provide a baseline of information about linker lengths appropriate for a 4/3 conotoxin. They are complementary to a recent study on the 4/3 conotoxin, ImI,[15] which showed

that short linkers tended to favor a non-native ribbon disulfide connectivity. Here, we show that longer linkers favor the native globular connectivity.

The systematic studies of linker length reported here show that differential effects are seen at the two main targets for RgIA, thus providing opportunities for tailoring selectivity. As the size of the linker increased, so too did the ability of the cyclic RgIA peptides to inhibit ACh-evoked currents at the $\alpha9\alpha10$ nAChR, with the most potent inhibitor at the $\alpha9\alpha10$ nAChR being cRgIA-7. This trend might be a consequence of longer linkers having greater flexibility and therefore reducing any residual strain on the main chain of the peptide. By contrast, the most potent cyclic analogue for $GABA_B$ receptor-dependent inhibition of HVA Ca^{2+} channel currents in rat DRG neurons was cRgIA-6, and increasing to a seven-residue linker had a detrimental effect on potency, increasing the IC_{50} nearly 10-fold from 4 nM to 36 nM. It appears that entropic effects contribute more to $GABA_B$ receptor-mediated Ca^{2+} channel current inhibition than to $\alpha9\alpha10$ nAChR-mediated binding and that excess flexibility in the ligand is, accordingly, energetically more costly. Thus, further improvements in $GABA_B$ targeting might be achieved by a more rigid six-residue linker, perhaps incorporating Pro as a conformationally constrained residue.

Interestingly, the linear peptide RgIA[ΔR] has potency similar to that of cRgIA-6 at the $GABA_B$ receptor, raising the possibility that removal of the terminal arginine might be responsible for the enhanced activity relative to the native peptide. However, cRgIA-7, which also lacks the arginine residue, has lower activity at the $GABA_B$ receptor, indicating that deletion of the arginine residue alone does not enhance potency. The negative charge of the C-terminal carboxyl is masked in RgIA[ΔR] since this peptide is amidated; therefore, comparisons between cyclic and linear molecules are not complicated by this factor. However, it would be interesting in future studies to deconvolute the role (if any) of terminal charge neutralization in the improved activity of cyclic derivatives.

Cyclization has been demonstrated to improve the stability of several conotoxin peptides;[8−10,15,39] therefore, the peptides examined here were tested in human serum to see if they had enhanced stability against degradation. There was an improvement in the stability of the cRgIA-6 and cRgIA-7 analogues relative to RgIA[ΔR], further supporting what has been found with other conotoxins and suggesting that cyclization should be a widely applicable approach to conotoxin stabilization. The improvement in stability brought about by cyclization appears to be a general phenomenon and is reflected in the exceptional stability of a large number of naturally occurring disulfide-rich macrocyclic peptides from bacteria, plants, and animals,[46] best exemplified by the disulfide-rich cyclotides.[47] Indeed, it was the natural head-to-tail cyclic backbone of these molecules that originally inspired the strategy to artificially cyclize conotoxins. The application of cyclization to other peptide toxins being explored for therapeutic benefits, such as toxins from snakes or scorpions, might also help in improving their stability. A recent study showed, for example, improvements in the serum stability of the scorpion toxin chlorotoxin, which when conjugated to a dye has been proposed as an imaging agent for defining the margins of brain tumors during surgery.[48] The cyclization approach is complementary to a range of other approaches that have been applied for optimizing conotoxin-based drug leads.[45] Finally, the in vivo effects of improving the stability of conotoxins via cyclization have not been widely studied, but cyclization of Vc1.1 was associated with the induction of orally delivered activity in an animal pain model,[10] so there is promise that improvements in oral activity might also be achieved for other peptides via cyclization. Further studies are required to establish if cyclization facilitates oral analgesic activity of RgIA, as it did for Vc1.1. We also note that additional studies on human receptors, rather than rat (or hybrid rat/human) receptors as studied here, will be necessary before a complete assessment of cyclic RgIA as a potential therapeutic can be made.

EXPERIMENTAL PROCEDURES

Synthesis and Cleavage of Mutants. Linear and cyclic peptide mutants were assembled on a rink amide MBHA resin (Novabiochem) and phenylacetamidomethyl resin, respectively, using manual solid-phase peptide synthesis with an in situ neutralization/2-(1*H*-benzotriazol-1-yl)-1,1,3,3,-tetramethyluronium hexafluorophosphate (HBTU) activation procedure for 9-fluorenylmethyloxycarbonyl and *tert*-butoxycarbonyl chemistry. All cyclic peptides were synthesized using acetamidomethyl (Acm) protection on Cys^{II} and Cys^{IV} to direct the folding into the correct globular conformation. The linkers were composed of small amino acids (Ala and Gly) arranged to avoid spectral degeneracy. Cleavage of the peptide from the resin was achieved by treatment with trifluoroacetic acid (TFA), triisopropylsilane (TIPS), and water as scavengers (9:0.5:0.5 TFA/TIPS/water). The reaction was allowed to proceed at room temperature (20−23 °C) for 2.5 h. The TFA was then evaporated, and the peptide was precipitated with ice-cold ether, filtered, dissolved in 50% solvent A/B (Solvent A: H_2O/0.05% TFA. Solvent B: 90% CH_3CN/10%H_2O/0.045% TFA), and lyophilized. *tert*-Butoxycarbonyl peptides were cleaved using hydrogen fluoride (HF) with *p*-cresol and *p*-thiocresol as scavengers [9:0.8:0.2 (vol/vol) HF/*p*-cresol/*p*-thiocresol] at −5 to 0 °C for 1.5 h. After cleavage, the peptide was precipitated with ether and then dissolved in 50% acetonitrile containing 0.05% trifluoroacetic acid (TFA) and lyophilized.

Crude peptides were purified by RP-HPLC on a Phenomenex C18 column using a gradient of 0−80% B in 80 min, with the eluent monitored at 215 and 280 nm. These conditions were used in subsequent purification steps unless stated otherwise. ES-MS confirmed the molecular mass of the fractions collected, and those displaying the correct mass were pooled and lyophilized for oxidation. All peptides were oxidized by dissolution in 0.1 M NH_4HCO_3 (pH 8.2) at a concentration of 0.3 mg/mL with stirring overnight at room temperature. For RgIA, 25% of propan-2-ol was added to the buffer. The peptides typically folded into one predominant form, which was apparent by RP-HPLC, and were purified using a gradient of 0−80% solvent B over 160 min. The 9-fluorenylmethyloxycarbonyl synthesized peptides were analyzed on analytical RP-HPLC and ES-MS to confirm the purity and molecular mass, and the disulfide connectivity was confirmed by NMR spectroscopy. For the *tert*-butoxycarbonyl synthesized Cys-Acm protected cyclic peptides, the Acm protecting group had to be removed to allow the second disulfide bond to form. For this step, the cyclic peptides were dissolved in 50% acetic acid (0.5 mg/mL) in the presence of 1 M HCl (0.1 mL/mg) and 0.1 M I_2 (in 50% acetic acid). The flask was flushed with nitrogen, and the reaction was left to proceed for 24 h. Ascorbic acid (1 M) was used to quench the reaction before another purification step on a 0−80% solvent B gradient over 160 min. If isomers could not be separated at this gradient, the samples were repurified on a 0−40% solvent B gradient over 160 min. All peptides were assessed to be of >95% purity using HPLC.

NMR Spectroscopy. NMR data for all peptides were recorded on Bruker Avance 500 and 600 MHz spectrometers, with samples dissolved in 90% H_2O/10% D_2O. Two dimensional NMR experiments included TOCSY and NOESY recorded at 280 K, pH 3.5, with mixing times of 80 and 350 ms, respectively. In preliminary experiments, NOE peak

intensities at a typically used mixing time for structure determination of 200 ms were found to be very weak. NOE build-up curves were thus measured (Supporting Information, Figure S1) to determine the optimal mixing time for obtaining distance information. The build-up curves indicated that a mixing time of 350 ms provided a good compromise between signal intensity and spin diffusion. Spin diffusion appeared to be negligible at this mixing time, which is still on the steep part of the NOE build-up curve. Spectra were analyzed using Topspin 1.3 (Bruker) and Sparky software.

Electrophysiological Recordings from nAChRs Expressed in *Xenopus* Oocytes. All oocytes were injected with 5 ng of cRNA of human α9 and rat α10 nAChR subunits and kept at 18 °C in ND96 buffer (96 mM NaCl, 2 mM KCl, 1 mM $CaCl_2$, 1 mM $MgCl_2$, and 5 mM HEPES, at pH 7.4) supplemented with 50 mg/L gentamicin and 5 mM pyruvic acid two to five days before recording. The human α9 clone was sourced from OriGene Technologies Inc. (Rockville, MD), and the rat α10 clone was a gift from Dr. A.B. Elgoyhen (Buenos Aires, Argentina). Human α10 clone was not available at the time the experiments were done. Membrane currents were recorded from *Xenopus* oocytes using a GeneClamp 500B amplifier (Molecular Devices, Sunnyvale, CA). Both the voltage-recording and the current-injecting electrodes were pulled from borosilicate glass (Harvard Apparatus Ltd., Edenbridge, UK) and had resistances of 0.3 to 1.5 MΩ when filled with 3 M KCl. All recordings were conducted at room temperature using a bath solution of ND96, as described above. During recordings, the oocytes were perfused continuously at a rate of 1.5 mL/min, with 300 s incubation times for the peptide. Acetylcholine (ACh) was applied for 2 s at 5 mL/min, with 3−5 min washout periods between applications. RgIA and the analogues were bath applied and coapplied with the agonist. Oocytes were voltage-clamped at a holding potential of −80 mV. The peak current amplitude was measured before and after incubation of the peptide.[49]

Electrophysiological Recordings from Dorsal Root Ganglia (DRG) Neurons. DRG neurons were enzymatically dissociated from ganglia of 7−14 day old Wistar rats as described previously.[11] Procedures for harvesting rat DRG were approved by the RMIT University Animal Ethics Committee. The external recording solution for rat DRG neurons contained (in mM) 150 TEACl, 2 $BaCl_2$, 10 D-glucose, and 10 HEPES; pH 7.3−7.4. Recording electrodes contained an internal solution consisting of (in mM) 140 CsCl, 1 $MgCl_2$, 5 MgATP, 0.1 NaGTP, 5 BAPTA-Cs_4, and 10 HEPES, pH 7.3, with CsOH and had resistances of 1.0−2.5 MΩ. Membrane currents were recorded using the whole-cell patch clamp recording technique with an Axopatch 200B amplifier (Molecular Devices). A voltage protocol using step depolarizations from −80 mV to −10 mV was used when examining high voltage-activated (HVA) Ca^{2+} channel currents. Test potentials 150 ms in duration were applied every 20 s. Leak and capacitative currents were subtracted using a −P/4 pulse protocol. Currents were generated using pClamp 9.2 software (Molecular Devices), filtered at 2 kHz, and sampled at 8 kHz by the Digidata 1322A (Molecular Devices). Sampled data were stored digitally for further analysis.

Stability Assays. Serum stability assays were carried out on male AB human serum (Sigma-Aldrich). Serum was centrifuged at 17,000*g* for 10 min, and the supernatant was removed and incubated for a further 10 min at 37 °C. Triplicate samples were prepared at a 1:10 dilution of peptide/serum with a working peptide concentration of 20 μM. Forty microliters of sample was removed at 0, 3, 5, 8, and 24 h and denatured in 40 μL of 6 M urea for 10 min at 5 °C. Forty microliters of 20% trichloroacetic acid (TCA) was then added for 10 min to precipitate the serum proteins at 5 °C. Samples were centrifuged at 14,000*g* for 10 min before analysis on a 0.3 mL/min Phenomenex column using a linear 1% gradient of 0−50% solvent B. Triplicate samples of peptide in PBS were also run for each time point as controls. An aliquot of the sample was injected, and the amount of intact peptide remaining was determined by integration at 215 nm.

■ ASSOCIATED CONTENT

Supporting Information. Supplementary figure showing NOE buildup curves vs mixing time to establish that NOEs are not dominated by spin diffusion at the mixing time used to derive distance restraint data for structural calculations. This material is available free of charge via the Internet at http://pubs.acs.org.

■ AUTHOR INFORMATION

Corresponding Author

*Tel: 61-7-3346 2019. Fax: 61-7-3346 2101. E-mail: d.craik@imb.uq.edu.au.

Present Addresses

[||]The University of Queensland, School of Biomedical Sciences, Brisbane, Australia, 4072.

■ ACKNOWLEDGMENT

Work in our laboratory on conotoxins is supported by a grant from the Australian Research Council (ARC) and the National Health and Medical Research Council (NHMRC). D.J.C. is an NHMRC Professorial Fellow. D.J.A. is an ARC Australian Professorial Fellow. R.J.C. is a NHMRC Biomedical CDA Fellow. N.L.D. is a Queensland Smart State Fellow. We gratefully acknowledge the assistance of Dr. Simon Nevin (QBI, University of Queensland) and access to the facilities of the ARC Special Research Centre for Functional and Applied Genomics.

■ ABBREVIATIONS USED

Acm, acetamidomethyl; ACh, acetylcholine; HVA, high voltage-activated; DRG, dorsal root ganglion; MBHA, 4-methylbenzhydrylamine; HBTU, 2-(1*H*-benzotriazol-1-yl)-1,1,3,3-tetramethyl uranium hexa fluorophosphates; TIPS, triisopropylsilane; HF, hydrogen fluoride; TFA, trifluoroacetic acid; ES-MS, electrospray mass spectrometry; TEAC1, tetraethylammonium chloride; HEPES, 4-(2-hydroxyethyl)-1-piperazineethanesulfonic acid; TOCSY, total correlation spectroscopy; NOESY, nuclear Overhauser enhancement spectroscopy; nAChR, nicotinic acetylcholine receptor; IC_{50}, half-maximal inhibitory concentration

■ REFERENCES

(1) Olivera, B. M.; Gray, W. R.; Zeikus, R.; McIntosh, J. M.; Varga, J.; Rivier, J.; de Santos, V.; Cruz, L. J. Peptide neurotoxins from fish-hunting cone snails. *Science* **1985**, *230*, 1338–1343.

(2) Adams, D. J.; Alewood, P. F.; Craik, D. J.; Drinkwater, R. D.; Lewis, R. J. Conotoxins and their potential pharmaceutical applications. *Drug Dev. Res.* **1999**, *46*, 219–234.

(3) Olivera, B. M. "Conus" venom peptides: reflections from the biology of clades and species. *Annu. Rev. Ecol. Syst.* **2002**, *33*, 25–47.

(4) Livett, B. G.; Sandall, D. W.; Keays, D.; Down, J.; Gayler, K. R.; Satkunanathan, N.; Khalil, Z. Therapeutic applications of conotoxins that target the neuronal nicotinic acetylcholine receptor. *Toxicon* **2006**, *48*, 810–829.

(5) Halai, R.; Craik, D. J. Conotoxins: natural product drug leads. *Nat. Prod. Rep.* **2009**, *26*, 526–536.

(6) Miljanich, G. P. Ziconotide: neuronal calcium channel blocker for treating severe chronic pain. *Curr. Med. Chem.* **2004**, *11*, 3029–3040.

(7) Audie, J.; Boyd, C. The synergistic use of computation, chemistry and biology to discover novel peptide-based drugs: The time is right. *Curr. Pharm. Des.* **2010**, *16*, 1380–6128.

(8) Clark, R. J.; Fischer, H.; Dempster, L.; Daly, N. L.; Rosengren, K. J.; Nevin, S. T.; Meunier, F. A.; Adams, D. J.; Craik, D. J. Engineering

stable peptide toxins by means of backbone cyclization: stabilization of the α-conotoxin MII. *Proc. Natl. Acad. Sci. U.S.A.* **2005**, *102*, 13767–13772.

(9) Lovelace, E. S.; Armishaw, C. J.; Colgrave, M. L.; Wahlstrom, M. E.; Alewood, P. F.; Daly, N. L.; Craik, D. J. Cyclic MrIA: a stable and potent cyclic conotoxin with a novel topological fold that targets the norepinephrine transporter. *J. Med. Chem.* **2006**, *49*, 6561–6568.

(10) Clark, R. J.; Jensen, J.; Nevin, S. T.; Callaghan, B. P.; Adams, D. J.; Craik, D. J. The engineering of an orally active conotoxin for the treatment of neuropathic pain. *Angew. Chem., Int. Ed.* **2010**, *49*, 6545–6548.

(11) Callaghan, B.; Haythornthwaite, A.; Berecki, G.; Clark, R. J.; Craik, D. J.; Adams, D. J. Analgesic α-conotoxins Vc1.1 and Rg1A inhibit N-Type calcium channels in rat sensory neurons via $GABA_B$ receptor activation. *J. Neurosci.* **2008**, *28*, 10943–10951.

(12) McIntosh, J. M.; Absalom, N.; Chebib, M.; Elgoyhen, A. B.; Vincler, M. α9 nicotinic acetylcholine receptors and the treatment of pain. *Biochem. Pharmacol.* **2009**, *78*, 693–702.

(13) Dutton, J. L.; Craik, D. J. α-Conotoxins: nicotinic acetylcholine receptor antagonists as pharmacological tools and potential drug leads. *Curr. Med. Chem.* **2001**, *8*, 327–344.

(14) Ellison, M.; Olivera, B. M. α-4/3 Conotoxins: phylogenetic distribution, functional properties, and structure-function insights. *Chem. Rec.* **2007**, *7*, 341–353.

(15) Armishaw, C. J.; Dutton, J. L.; Craik, D. J.; Alewood, P. F. Establishing regiocontrol of disulfide bond isomers of alpha-conotoxin ImI via the synthesis of N-to-C cyclic analogs. *Biopolymers* **2010**, *94*, 307–313.

(16) Ellison, M.; Haberlandt, C.; Gomez-Casati, M. E.; Watkins, M.; Elgoyhen, A. B.; McIntosh, J. M.; Olivera, B. M. α-RgIA: a novel conotoxin that specifically and potently blocks the α9α10 nAChR. *Biochemistry* **2006**, *45*, 1511–1517.

(17) Franco, A.; Pisarewicz, K.; Moller, C.; Mora, D.; Fields, G.; Marì, F. Hyperhydroxylation: A New Strategy for Neuronal Targeting by Venomous Marine Molluscs. In *Molluscs*; Springer: Berlin, Germany, 2006; pp 83−103.

(18) Ellison, M.; Feng, Z. P.; Park, A. J.; Zhang, X.; Olivera, B. M.; McIntosh, J. M.; Norton, R. S. α-RgIA, a novel conotoxin that blocks the α9α10 nAChR: structure and identification of key receptor-binding residues. *J. Mol. Biol.* **2008**, *377*, 1216–1227.

(19) Vincler, M.; Wittenauer, S.; Parker, R.; Ellison, M.; Olivera, B. M.; McIntosh, J. M. Molecular mechanism for analgesia involving specific antagonism of α9α10 nicotinic acetylcholine receptors. *Proc. Natl. Acad. Sci. U.S.A.* **2006**, *103*, 17880–17884.

(20) Elgoyhen, A. B.; Johnson, D. S.; Boulter, J.; Vetter, D. E.; Heinemann, S. α9: An acetylcholine receptor with novel pharmacological properties expressed in rat cochlear hair cells. *Cell* **1994**, *79*, 705–715.

(21) Elgoyhen, A. B.; Vetter, D. E.; Katz, E.; Rothlin, C. V.; Heinemann, S. F.; Boulter, J. α10: A determinant of nicotinic cholinergic receptor function in mammalian vestibular and cochlear mechanosensory hair cells. *Proc. Natl. Acad. Sci. U.S.A.* **2001**, *98*, 3501–3506.

(22) Sgard, F.; Charpantier, E.; Bertrand, S.; Walker, N.; Caput, D.; Graham, D.; Bertrand, D.; Besnard, F. A. Novel human nicotinic receptor subunit, α10, that confers functionality to the α9-subunit. *Mol. Pharmacol.* **2002**, *61*, 150–159.

(23) Colomer, C.; Olivos-Ore, L. A.; Vincent, A.; McIntosh, J. M.; Artalejo, A. R.; Guerineau, N. C. Functional characterization of α9-containing cholinergic nicotinic receptors in the rat adrenal medulla: implication in stress-induced functional plasticity. *J. Neurosci.* **2010**, *30*, 6732–6742.

(24) Kaupmann, K.; Huggel, K.; Heid, J.; Flor, P. J.; Bischoff, S.; Mickel, S. J.; McMaster, G.; Angst, C.; Bittiger, H.; Froestl, W.; Bettler, B. Expression cloning of $GABA_B$ receptors uncovers similarity to metabotropic glutamate receptors. *Nature* **1997**, *386*, 239–246.

(25) White, J. H.; Wise, A.; Marshall, F. H. Heterodimerization of gamma-aminobutyric acid B receptor subunits as revealed by the yeast two-hybrid system. *Methods* **2002**, *27*, 301–310.

(26) Jones, K. A.; Borowsky, B.; Tamm, J. A.; Craig, D. A.; Durkin, M. M.; Dai, M.; Yao, W.-J.; Johnson, M.; Gunwaldsen, C.; Huang, L.-Y.; Tang, C.; Shen, Q.; Salon, J. A.; Morse, K.; Laz, T.; Smith, K. E.; Nagarathnam, D.; Noble, S. A.; Branchek, T. A.; Gerald, C. $GABA_B$ receptors function as a heteromeric assembly of the subunits GABABR1 and GABABR2. *Nature* **1998**, *396*, 674–679.

(27) Kaupmann, K.; Malitschek, B.; Schuler, V.; Heid, J.; Froestl, W.; Beck, P.; Mosbacher, J.; Bischoff, S.; Kulik, A.; Shigemoto, R.; Karschin, A.; Bettler, B. $GABA_B$-receptor subtypes assemble into functional heteromeric complexes. *Nature* **1998**, *396*, 683–687.

(28) Kuner, R.; Kohr, G.; Grunewald, S.; Eisenhardt, G.; Bach, A.; Kornau, H. C. Role of heteromer formation in $GABA_B$ receptor function. *Science* **1999**, *283*, 74–77.

(29) Ng, G. Y. K.; Clark, J.; Coulombe, N.; Ethier, N.; Hebert, T. E.; Sullivan, R.; Kargman, S.; Chateauneuf, A.; Tsukamoto, N.; McDonald, T.; Whiting, P.; Mezey, E.; Johnson, M. P.; Liu, Q.; Kolakowski, L. F., Jr.; Evans, J. F.; Bonner, T. I.; O'Neill, G. P. Identification of a $GABA_B$ receptor subunit, gb2, required for functional $GABA_B$ receptor activity. *J. Biol. Chem.* **1999**, *274*, 7607–7610.

(30) Dutar, P.; Nicoll, R. A. A physiological role for $GABA_B$ receptors in the central nervous system. *Nature* **1988**, *332*, 156–158.

(31) Bettler, B.; Kaupmann, K.; Mosbacher, J.; Gassmann, M. Molecular structure and physiological functions of $GABA_B$ receptors. *Physiol. Rev.* **2004**, *84*, 835–867.

(32) Pinard, A.; Seddik, R.; Bettler, B. $GABA_B$ Receptors: Physiological Functions and Mechanisms of Diversity. In *Advances in Pharmacology*; Blackburn, T. P., Ed.; Academic Press: San Diego, CA, 2010; Vol. 58, pp 231−255.

(33) Clark, R. J.; Daly, N. L.; Halai, R.; Nevin, S. T.; Adams, D. J.; Craik, D. J. The three-dimensional structure of the analgesic α-conotoxin, RgIA. *FEBS Lett.* **2008**, *582*, 597–602.

(34) Wishart, D. S.; Sykes, B. D. Chemical Shifts As a Tool for Structure Determination. In *Methods in Enzymology*; James, T. L., Oppenheimer, N. J., Eds.; Academic Press: San Diego, CA, 1994; Vol. 239, pp 363−392.

(35) Marx, U. C.; Daly, N. L.; Craik, D. J. NMR of conotoxins: structural features and analysis of chemical shifts of posttranslationally modified amino acids. *Magn. Reson. Chem.* **2006**, *44*, 41–50.

(36) Hutchinson, E. G.; Thornton, J. M. PROMOTIF: a program to identify and analyze structural motifs in proteins. *Protein Sci.* **1996**, *5*, 212–220.

(37) Laskowski, R. A. PROCHECK: a program to check the stereochemical quality of protein structures. *J. Appl. Crystallogr.* **1993**, *26*, 283–291.

(38) Callaghan, B.; Adams, D. J. Analgesic alpha-conotoxins Vc1.1 and RgIA inhibit N-type calcium channels in sensory neurons of α9 nicotinic receptor knockout mice. *Channels (Austin)* **2010**, *4*, 51–54.

(39) Armishaw, C. J.; Jensen, A. A.; Balle, L. D.; Scott, K. C.; Sorensen, L.; Stromgaard, K. Improving the stability of α-conotoxin AuIB through N-to-C cyclization: the effect of linker length on stability and activity at nicotinic acetylcholine receptors. *Antioxid. Redox Signaling* **2011**, *14*, 65–76.

(40) Kaas, Q.; Westermann, J.-C.; Craik, D. J. Conopeptide characterization and classifications: An analysis using ConoServer. *Toxicon* **2010**, *55*, 1491–1509.

(41) Nicke, A.; Loughnan, M. L.; Millard, E. L.; Alewood, P. F.; Adams, D. J.; Daly, N. L.; Craik, D. J.; Lewis, R. J. Isolation, structure, and activity of GID, a novel α-4/7-conotoxin with an extended N-terminal sequence. *J. Biol. Chem.* **2003**, *278*, 3137–3144.

(42) Blanchfield, J.; Dutton, J.; Hogg, R.; Craik, D.; Adams, D.; Lewis, R.; Alewood, P.; Toth, I. The synthesis and structure of an N-terminal dodecanoic acid conjugate of α-conotoxin MII. *Lett. Pept. Sci.* **2001**, *8*, 235–239.

(43) Blanchfield, J. T.; Dutton, J. L.; Hogg, R. C.; Gallagher, O. P.; Craik, D. J.; Jones, A.; Adams, D. J.; Lewis, R. J.; Alewood, P. F.; Toth, I. Synthesis, structure elucidation, *in vitro* biological activity, toxicity, and Caco-2 cell permeability of lipophilic analogues of α-conotoxin MII. *J. Med. Chem.* **2003**, *46*, 1266–1272.

(44) Green, B. R.; Catlin, P.; Zhang, M. M.; Fiedler, B.; Bayudan, W.; Morrison, A.; Norton, R. S.; Smith, B. J.; Yoshikami, D.; Olivera, B. M.; Bulaj, G. Conotoxins containing nonnatural backbone spacers: cladistic-based design, chemical synthesis, and improved analgesic activity. *Chem. Biol.* **2007**, *14*, 399–407.

(45) Bulaj, G. Integrating the discovery pipeline for novel compounds targeting ion channels. *Curr. Opin. Chem. Biol.* **2008**, *12*, 441–447.

(46) Craik, D. J. Chemistry. Seamless proteins tie up their loose ends. *Science* **2006**, *311*, 1563–1564.

(47) Craik, D. J.; Cemazar, M.; Wang, C. K.; Daly, N. L. The cyclotide family of circular miniproteins: nature's combinatorial peptide template. *Biopolymers* **2006**, *84*, 250–266.

(48) Akcan, M.; Stroud, M.; Hansen, S. J.; Clark, R. J.; Daly, N. L.; Craik, D. J.; Olson, J. Chemical re-engineering of chlorotoxin improves bioconjugation properties for tumor imaging and targeted therapy. *J. Med. Chem.* **2010**, *54*, 782–787.

(49) Nevin, S. T.; Clark, R. J.; Klimis, H.; Christie, M. J.; Craik, D. J.; Adams, D. J. Are $\alpha 9\alpha 10$ nicotinic acetylcholine receptors a pain target for alpha-conotoxins? *Mol. Pharmacol.* **2007**, *72*, 1406–1410.

(50) Gehrmann, J. G.; Alewood, P. F; Craik, D. J. Structure determination of the three disulfide bond isomers of α-conotoxin GI: a model for the role of disulfide bonds in structural stability. *J. Mol. Biol.* **1998**, *278*, 401–415.